OPTIMIZATION OF A CITRUS CANOPY SHAKER HARVESTING SYSTEM: MECHANISTIC TREE DAMAGE AND FRUIT DETACHMENT MODELS

S. K. Gupta, R. Ehsani, N. H. Kim

ABSTRACT. *Mechanization of fruit and nut harvesting is becoming increasingly important because of a significant rise in the cost of manual harvesting. This work proposes a progressive analytical approach for the design and optimization of a citrus canopy shaker harvesting machine. The approach was formulated using finite element (FE) methods to find the optimum design parameters of the machine. The design parameters were defined in terms of a configuration (or stiffness) of shaking rods and two operating parameters: shaking frequency and shaking amplitude. The formulated methodology consists of determining the properties of wood, statistical modeling of the tree limbs, developing mechanistic models, and performing optimization using FE simulations. The proposed methodology employs the response surface methodology or surrogate models to quantify the objective functions, and Pareto-optimal search techniques to find the optimum designs. Three sets of machine parameters were proposed in this study to minimize tree damage and maximize fruit removal. These optimal parameters were proposed based on the configuration and distribution of limbs and fruits in a medium-size citrus tree. The optimized tine configuration of the middle and bottom section of the canopy shaker consists of a solid rod made of polyamide reinforced with 50% long glass fibers and a hollow tube made of hardened steel in a 3:1 ratio by length. These tines, when vibrating at a high frequency of 7.8 Hz and low amplitude of 3.81 to 5.08 cm (1.5 to 2 in.) and a low frequency of 3 to 3.5 Hz and high amplitude of 13.9 to 15.2 cm (5.5 to 6 in.), provide a 25% to 30% reduction in damage to the tree limbs in the bottom and middle zones of the tree. Similarly, changes to the top sections of the canopy shaker with another set of optimized tine configurations resulted in a 40% to 45% reduction in the damage to the limbs of the top section of the tree canopy. The optimized tine configuration, thus proposed for the top section of the canopy shaker, is made of a solid rod of polyamide reinforced with 60% long glass fibers and vibrates at a frequency of 6.5 to 7.5 Hz with an amplitude of 7.6 to 8.9 cm (3 to 3.5 in.).*

Keywords. *Canopy shaker, Finite element analysis, Fruit detachment, Pareto frontier, Polynomial response surface.*

Mechanical harvesting equipment is becoming increasingly important in the fruit and nut industries due to the rising cost of production and lack of manual labor. The timely adaptation of technological advancements and innovation in mechanical harvesting is of utmost importance to the fruit and nut industries to ensure their sustainability. Most of the earlier work in designing mechanical harvesters for fruit crops was based on field trials and experimentation, which is tedious, time-consuming, and expensive. A procedure that is based on computer-assisted numerical methods could potentially increase the performance of a harvester and reduce the overall expense of the design.

The Florida citrus industry is a $9 billion industry, and citrus production encompasses an area of 2,151 km^2 (531,493 acres) in the state of Florida (FASS, 2013). The type of mechanical harvesting system currently used in Florida is the continuous canopy shaker. Even though the current design of canopy shakers has high harvesting efficiency (96% to 99%), growers are reluctant to use these machines due to their concern about significant damage to the main scaffold branches of the citrus trees, which can potentially affect the next year's yield. Therefore, to increase the use of mechanical harvesting for citrus crops, the problem of structural damage to the tree must be addressed by either modifying the existing design or by developing altogether a new design. This study proposes a methodology to modify the existing design using optimization techniques. Since the canopy shaker has to be optimized for the two conflicting objectives, i.e., to minimize tree damage and maximize the fruit removal, a multi-objective design approach has been employed. The most widely accepted procedure to solve multi-objective problems is the Pareto-optimal solution search technique (Pareto, 1906).

The Pareto-optimal solution guarantees that moving from the optimal solution, no improvement can be achieved in any of the objective functions without worsening others (Deb, 2001). The Pareto technique requires a significantly high number of function evaluations to solve a multi-objective

Submitted for review in June 2014 as manuscript number MS 10819; approved for publication by the Machinery Systems Community of ASABE in March 2016.

The authors are **Susheel K. Gupta,** Graduate Student, and **Reza Ehsani, ASABE Member,** Associate Professor, University of Florida Citrus Research and Education Center, Lake Alfred, Florida, and **Nam-Ho Kim,** Associate Professor, Department of Mechanical and Aerospace Engineering, University of Florida, Gainesville, Florida. **Corresponding author:** Reza Ehsani, 700 Experiment Station Road, Lake Alfred, FL 33850; phone: 863-956-1151, ext. 1228; e-mail: ehsani@ufl.edu.

Vol. 59(4): 761- 776 ISSN 2151-0032 DOI 10.13031/trans.59.10819

optimization problem. Thus, a computationally efficient strategy should be employed in the optimization of such problems. One of the most effective approaches to minimize the cost of optimization in recent years is founded on response surface methodology (RSM) (Myers and Montgomery, 2002). RSM approximates the real objective functions using a design of experiments (DOE) model. The intent of the DOE is to characterize the system response using a minimum number of actual analysis runs. When the DOE is complete, the response surface functions are fit to the analysis data and serve as a surrogate model. The optimization algorithm then samples the surrogate model to search for the optimal design. As a result, the optimization runs quickly because it is sampling the surrogate model instead of solving each point deterministically.

The following steps should be developed in order to implement a multi-objective approach using RSM:

- Identify and quantify the objective functions.
- Define design variables.
- Model a proper DOE.
- Define and verify the finite element (FE) or numerical method.
- Evaluate objective functions in the DOE using the FE method.
- Construct RSM (also called surrogate models or metamodels).
- Formulate multi-objective optimization to determine the Pareto-optimal solutions.

The most significant part in the design optimization of the canopy shaker is to identify and properly quantify the objective functions. Many methods are suggested in the literature; however, this study employs a mechanistic model to quantify the objective functions. Veletsos and Newmark (1960) applied these concepts to formulate a damage index in terms of the ductility ratio, defined as the ratio of the maximum deformation to the yield deformation. Lybas and Sozen (1977) proposed a similar model to estimate the damage potential in structures using the ratio of the pre-yield stiffness to the secant stiffness corresponding to the maximum deformation. Park and Ang (1985) proposed a mechanistic model that evaluates the structural damage in reinforced concrete structures due to earthquake ground motions. The damage was expressed as a linear function of the maximum deformation and the effect of repeated cyclic loading. Roufaiel and Meyer (1987) defined a damage index based on the flexural flexibility, which is the ratio of the rotation to moment before and after an earthquake and the ultimate flexibility. Powell and Allahabadi (1988) presented two concepts for damage assessment: one was based on demand versus capacity, and the other was based on the degradation of structural properties. The demand versus capacity assessment included strength, displacement, deformation, and energy dissipation, whereas the degradation concept used degradation in stiffness, strength, and energy dissipation capacity.

Numerical tools have been successfully employed to automate the design optimization of aeronautical and automobile structures (Arora, 1995; Baier, 1977; Leitmann, 1977; Stadler, 1988, 1992; Koski, 1979, 1980; Carmichael, 1980, Choi and Kim, 2005a, 2005b). With the development of the finite FE method, the use of numerical techniques has increased and gained popularity to efficiently solve complex optimization problems in many fields (Kristensen and Madsen, 1976; Pedersen and Laursen, 1983; Santos and Choi, 1989; Bathe, 1996; Kim, 2009). Many engineering problems in the area of structural design consist of more than one objective, thus requiring special numerical techniques to find the cost-effective solution of the optimization. Marler and Arora (2004) described the main characteristics, advantages, and drawbacks of various numerical and random methods used to solve multi-objective problems. Messac et al. (2003) provided a review and comparison of several multi-objective algorithms based on numerical optimization. Das and Dennis (1997), Cheng and Li (1998), Das and Dennis (1998), and Messac and Ismail-Yahaya (2003) have respectively developed the weighted-sum algorithm, compromise programming, normal boundary intersection method, and normalized normal constraint method to find optimal designs using multi-objective optimization.

Computer simulation has been used in the past by Phillips et al. (1970), Fridley and Yung (1975), and Savary et al. (2010) to design mechanical harvesters. However, the current study presents an economical way to design a harvester using statistical models of limb prototypes, finite element methods, and response surface based design optimization. A progressive design approach has been adopted in this research that involves determining the properties of wood, accumulating and organizing statistical information for modeling tree limbs, quantifying objective functions using mechanistic models, modeling machine-tree interaction, performing dynamic analysis using finite element analysis (FEA), and predicting the optimized designs. The mechanical and physical properties of citrus wood and the modeling and classification of the limb prototypes into the three different zones of the tree canopy were discussed in the first part of this research (Gupta et al., 2015), and the rest of the design approach is presented in this article.

Increasing the shaking force uniformly to all the parts of a citrus tree will increase the fruit removal; however, this will also cause a great amount of tree damage. A citrus tree canopy has a non-uniform architecture with varying density of fruits and primary limbs (main scaffold branches), as shown in figure 1. If a shaker is designed such that it provides higher shaking force to the tree limbs where it is most required, that is, in the fruiting region of the canopy, and low

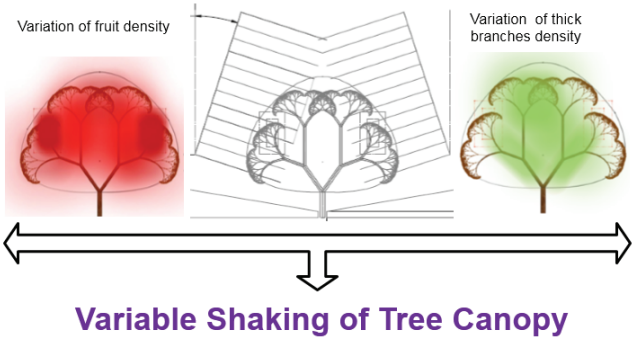

Figure 1. Pictorial view showing the variation in the fruit density and thick branches of a citrus tree and how the shaker interacts with the tree canopy.

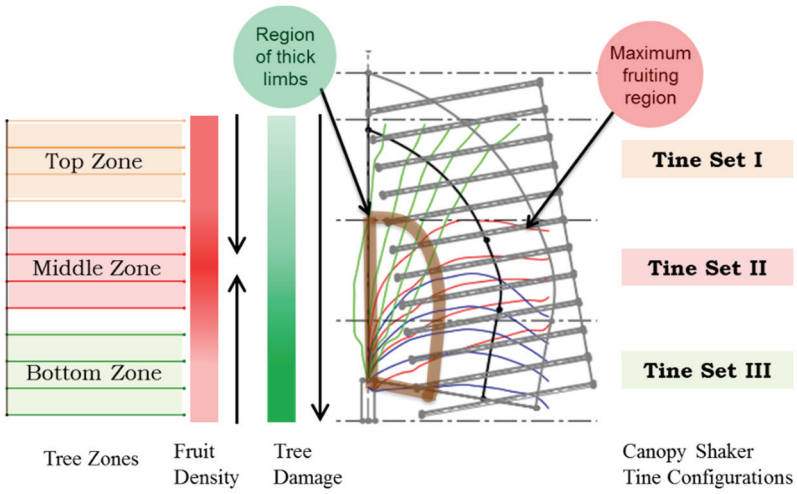

Figure 2. Three machine configurations (tine sets I, II, and III) of the canopy shaker corresponding to three zones of a citrus canopy (top zone, middle zone, and bottom zone, respectively).

shaking force where the likelihood of breaking the main scaffold branches is higher, then it would result in a considerable reduction in tree damage without significantly affecting the fruit removal efficiency. The proposed study employed this idea of variable shaking of the citrus canopy to improve the performance of the canopy shaker harvester. To implement the variable shaking, the citrus canopy is divided into three zones (Gupta et al., 2015). Correspondingly, the shaking mechanism is divided into three sections (tine sets I, II, and III), as shown in figure 2. These three sections have different shaking parameters, such as tine stiffness, frequency, and amplitude of vibration. This research is limited in that it proposes only three different sets of tines or machine configurations in order to control the cost of the canopy shaker.

Materials and Methods

The FE model was developed in Abaqus (ver. 6.10, Dassault Systèmes Simulia Corp., Providence R.I.) to simulate the dynamic response of the tree limb prototypes. The FE model was validated using laboratory test equipment. The principles of mechanistic models were employed to formulate the objective functions for tree damage and fruit removal efficiency. These two conflicting objective functions required the formulation of a multi-objective optimization. The Pareto-optimal technique was used to determine the optimal machine/tine configuration of a canopy shaker.

Finite Element Model

The principal mechanism to detach citrus fruits involves impacting the tree limbs repeatedly with a vibrating tine, a rod-like structure attached to the machine. In Oxbo citrus canopy shakers (models 3220 and 3210, Oxbo International, Shipshewana, Ind.), the tines are 1.8 m long and mounted on a wheel-like structure called a hub, as shown in figure 3a. Each hub is designed to rotate freely on a vertical axis, as shown in figure 3b. The canopy shaker has 12 hubs of tines, each having 16 tines. In addition to the vibratory motion of the tine-hub assembly, the shaker continuously moves in the forward direction to accomplish mass harvesting. Mechanical harvesting is a complex phenomenon that involves the interaction between the machine and tree, as well as interactions among the different parts of the tree, such as fruits, branches, and leaves. Therefore, some assumptions and generalizations have to be made to efficiently model and simulate the physical phenomena.

The tine, a critical part of a canopy shaker that directly interacts with trees, is the only machine component modeled in the FEA. The tine was modeled as a 3D linear elastic two-node cantilever beam and meshed to 100 finite elements. Based on information from Florida citrus growers and studies by Roka et al. (2008), it was noted that the canopy shaker travels at an average speed of 0.223 m s^{-1} (0.5 mph), and the hub rotates at an approximate speed of one cycle per minute. Therefore, in the FEA, the tine is subjected to a forward speed of 0.223 m s^{-1} and an angular speed of 0.105 rad s^{-1} in addition to its sinusoidal vibration, as shown in figure 3b. The analyses were run for 1 s as the tines were found to interact with the tree limbs for about that length of time.

Because of the non-uniformity and randomness of the tree architecture, instead of analyzing the whole tree, this research used limb prototypes, which are non-physical representations of actual tree limbs and are determined statistically. The statistical derivation of limb prototypes from actual primary limbs was explained by Gupta et al. (2015). These limbs were modeled as 3D linear elastic two-node cantilever beams with tapered circular cross-sections and meshed to 160 finite elements to appropriately balance the accuracy and computation time. In this study, main scaffold branches originating from the trunk of a tree and having a base diameter greater than 6.35 cm (2.5 in.) are classified as primary limbs, whereas branches originating from a primary limb and having a base diameter greater than 2.54 cm (1 in.) and less than 6.35 cm (2.5 in.) are called secondary branches. The effects of secondary branches, fruits, and leaves, and their mutual interactions, should be modeled in order to accurately simulate the physical phenomena. However, such analysis would be very complex and prohibitively expensive; thus, some assumptions have been made in this study

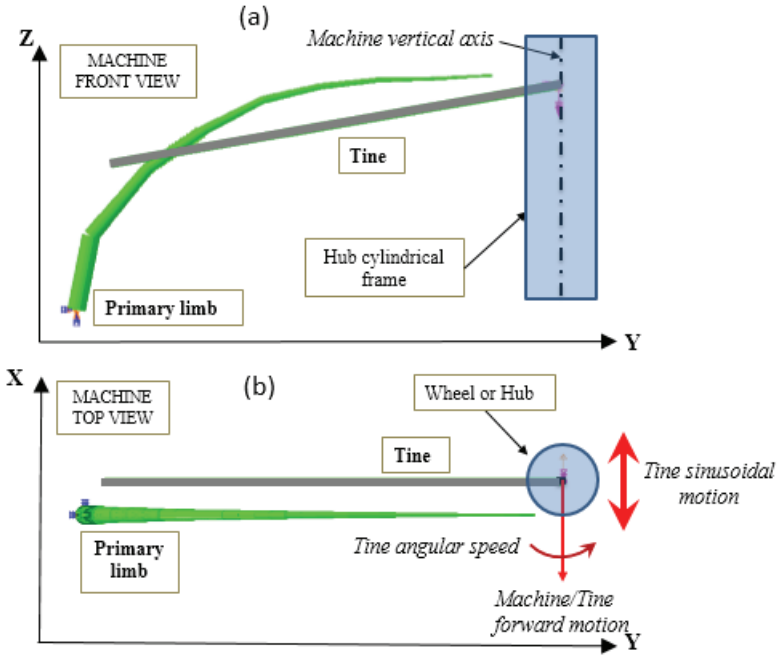

Figure 3. (a) Finite element model of a tree limb and tine modeled using beam elements and (b) boundary conditions and how the tine interacts with the primary limb in the FEA model.

to approximately model them. Secondary branches and fruits were modeled by aggregating their masses on the primary limbs, as explained by Gupta et al. (2015). Figure 4 shows the 50th percentile limb prototype or representative of the middle zone lumped with the mass of the secondary branches and fruits.

It was noted that the tine repeatedly strikes the branches and forces them vibrate freely at their natural frequency. However, as soon as the distance between the branches and the tine decreases due to forward motion of the canopy shaker, the tine starts bending the branches, and may break them eventually. This physical interaction between tine and the branches is also modeled in the FEA and defined using the non-sticky (or rough separation) contact between the branch and the tine.

The individual interactions of the secondary branches, twigs, leaves, and fruits with the machine and among themselves are not included in the scope of this study. However, their combined effect, which attenuates the dynamic response of the limbs, was measured experimentally (Gupta et al., 2015) and is modeled as Rayleigh damping, as shown in equation 1:

$$[C]=\alpha[M]+\beta[K] \quad (1)$$

where M, K, and C are the mass, stiffness, and damping matrices of a system, respectively; α is mass-proportional damping; and β is stiffness-proportional damping. It was noted that the damping ratio of trees is largely viscous and mostly depends on the mass of the main branches, secondary branches, and fruits (Moore, 2002). Therefore, mass-proportional damping was used in this study to account for the overall damping. Based on the parametric studies of the limb prototypes corresponding to the 50th percentile of each zone, a value of 87.25 s^{-1} was set for α, and a low value of 0.0001 s was set for β rather than a null value (Mayer, 1987) to mitigate the numerical noise.

In the canopy shaker, the tine vibrates at certain frequency and repeatedly impacts the branch for certain duration to accomplish harvesting. The number of impacts and the instantaneous time of the impacts should be calculated in order to accurately determine the dynamic response of the limbs. After the first strike, the branch starts vibrating at higher modes, and thus causes the next impact parameters to be determined based on the vibration modes of both tine and branch. The analytical formulation to model this phenomenon is complex and tedious to solve; thus, an FEA is used to simulate the non-linear dynamic behavior of a limb under repeated impacts from a tine.

An isotropic elastic material model is considered for both the tree limb and the tine. The mechanical and physical properties of citrus wood were set based on results obtained from laboratory experiments on green citrus wood samples (Gupta

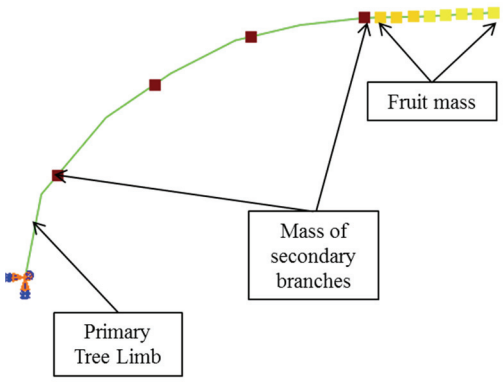

Figure 4. Finite element model with secondary branches (brown squares) and fruits (yellow squares) modeled as lumped masses on a primary limb.

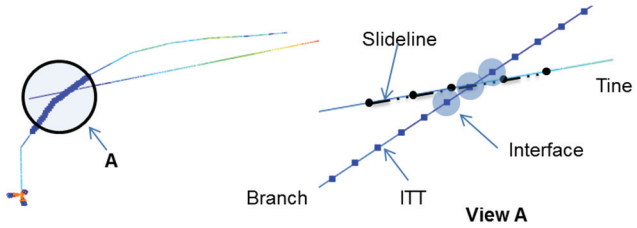

Figure 5. Interaction of tine and branch using Abaqus ITT elements.

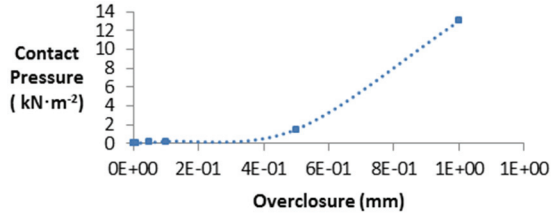

Figure 6. Pressure-overclosure relationship to define normal contact behavior between tine and primary limb during impact.

et al., 2015; Savary et al., 2010). The interaction between the tree limb and the tine, which results in their dynamic motions when they come into contact, was defined using Abaqus tube-to-tube elements (ITT3), as shown in figure 5. Normal contact behavior is defined using the tabular piecewise-linear pressure-overclosure relationship to simulate the soft impact condition between the tine and the primary limb, as shown in figure 6. This condition allows a small amount of penetration into the branch to resolve the numerical difficulties encountered in the simulation. The tangential behavior of the contact was modeled by the classical isotropic coulomb friction model with a coefficient of friction of 0.36 (Gupta et al., 2015). The non-linear dynamic response of the branch was analyzed using an implicit direct integration with a Hilber-Hughes-Taylor operator (Hilber et al., 1977; Hughes, 1987) having α_1, β_1, and γ_1 values of -0.05, 0.275625, and 0.55, respectively. Abaqus direct based on the Lagrange multiplier and the Abaqus penalty method were used to enforce the pressure-overclosure constraint and the frictional constraint, respectively.

Verification and Validation of Finite Element Model

The tree limb prototypes used to optimize the canopy shaker are non-physical limbs and are derived from statistical data; therefore, it is not possible to experimentally verify the FE parameters using the limb prototypes. An alternative method was devised to verify the parameters of the FE model so as to accurately simulate the physical phenomena in canopy shaker harvesting. A small-scale setup that used the same vibratory mechanism as that of the canopy shaker was developed. The dynamic responses of tree limbs were measured in terms of longitudinal normal strain and acceleration and then compared with the FE simulation.

The laboratory test equipment used a slider crank mechanism and was built in-house, as shown in figure 7. An electric motor powers the piston of the test equipment to oscillate the tine with a stroke of 2.54 cm (1 in.). The branch and tine were installed to form a cross-shaped assembly. To approximately simulate orchard conditions during canopy shaking, three values of clearance, i.e., 0.0 cm (0 in.), 1.27 cm (0.5 in.), and 2.54 cm (1 in.), were set between the tine and the branch by adjusting the movable clamp in the *z*-direction, as shown in figure 8. The section of tine at 17.78 cm (7 in.) from its free end was set to strike the branch at two locations, i.e., 50.8 cm (20 in.) and 88.9 cm (35 in.), from the fixed end of the branch. The experiments were conducted at vibrational frequencies of 2.4, 3.8, 5.1, and 6.5 Hz.

A galvanized metal tube mounted along the *y*-axis and having an outer diameter of 1.746 cm (11/16 in.), wall thickness of 0.159 cm (0.0625 in.), length of 71.120 cm (28 in.), and weight of ~0.318 kg (0.7 lb) was used as the time to impact the branch in the laboratory experiment. A branch specimen that was free of disease, burrs, swelling, and cracks was cut from a Valencia orange tree growing at the University of Florida CREC research orchard. The branch specimen was 177.8 cm (70 in.) long with a maximum diameter of 1.667 cm (21/32 in.) at the fixed end, minimum diameter of 1.111 cm (7/16 in.) at the tip, and weight of 0.385 kg (0.85 lb). During the experiment, the branch specimen was mounted along the positive *x*-axis, with the larger-diameter end fixed to the solid frame using an adjustable clamp, as shown in figure 8.

Acceleration Acquisition

A set of accelerometers (Freescale, 2008), shown in figure 7, were mounted on the branch specimen at distance of 76.2 cm (30 in.) and 152.4 cm (60 in.) from its fixed end. Data were acquired using a Compact DAQ system (model NI 96211, National Instruments Inc., Tex.). A LabView program was designed to acquire acceleration data from the accelerometers at a sampling rate of 100 Hz. The acceleration was computed using equation 2:

$$\text{Acceleration}\,(a) = \frac{\text{Sensor reading} - \text{Sensor reading corresponding to 0 } g}{\text{Sensitivity of the accelerometer}} \times 9.8\ \text{m s}^{-2} \quad (2)$$

Strain Acquisition

Strain gauges (350 Ω, Micro-Measurements, Wendell, N.C.), shown in figure 9, were installed per ASTM Standard E1237-93 (ASTM, 2014) on both the top and bottom surfaces of the branch near the fixed end to continuously record tensile and compressive longitudinal strains. The LabView Virtual Instrument (National Instrument, Austin, Tex.) was designed to communicate between the strain gauges and the data acquisition (DAQ) system. Data were acquired at a sampling rate of 1,000 Hz using a quarter bridge strain gauge module (model NI 9236, National Instruments, Austin, Tex.). Two different cantilever loads of 0.02 and 0.26 kg were applied at the end of the branch specimen to theoretically verify the readings from the strain gauges. The strain verification test was repeated three times at different intervals during the laboratory test, and results were compared to ensure the consistency of the installed strain gauges.

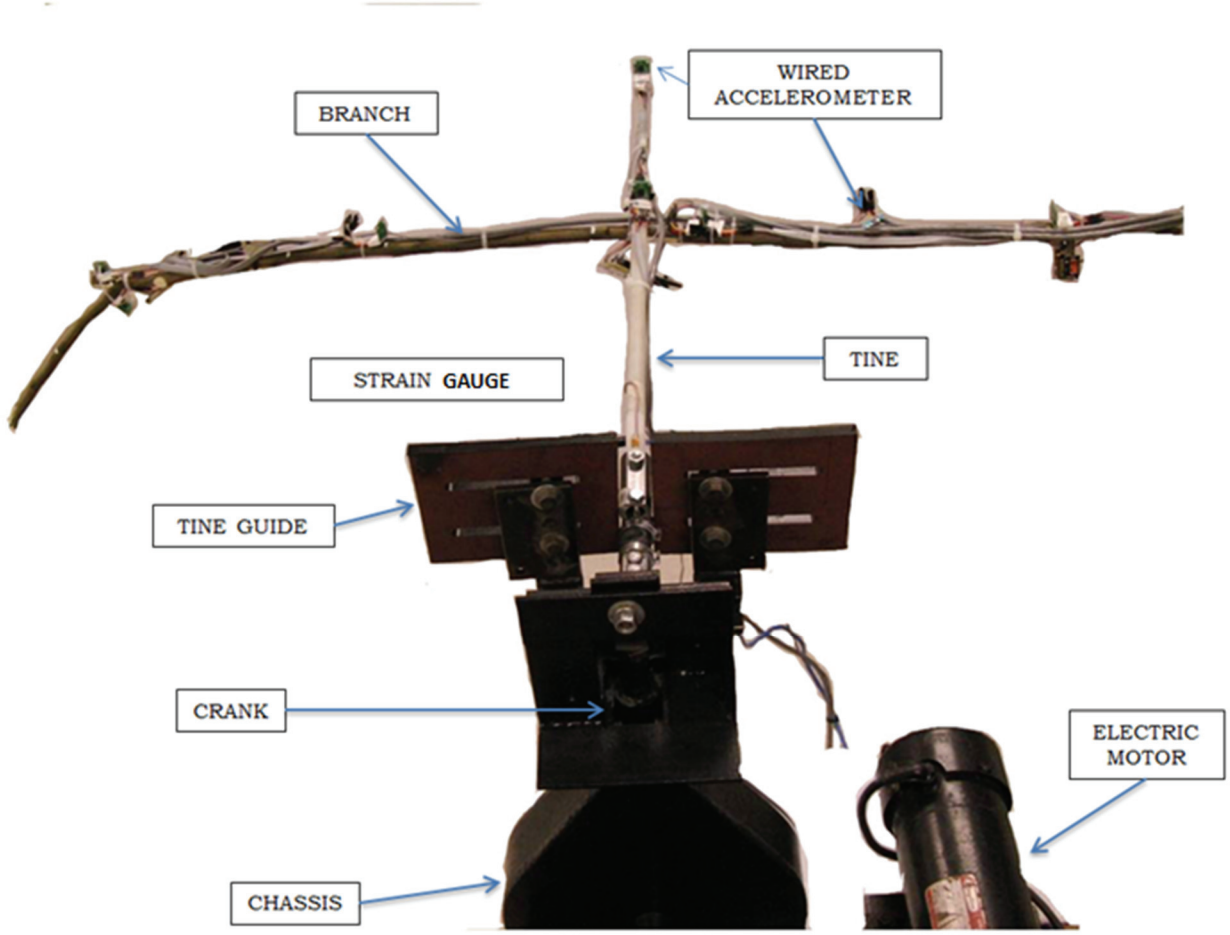

Figure 7. Schematic of laboratory test equipment used to validate the FE model parameters.

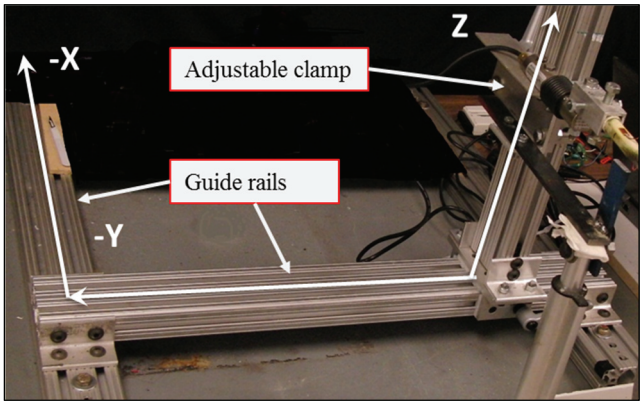

Figure 8. Branch specimen fixed to the solid frame with a movable bracket and clamp. The frame can be adjusted along the *x* and *y* axes with the help of guide rails.

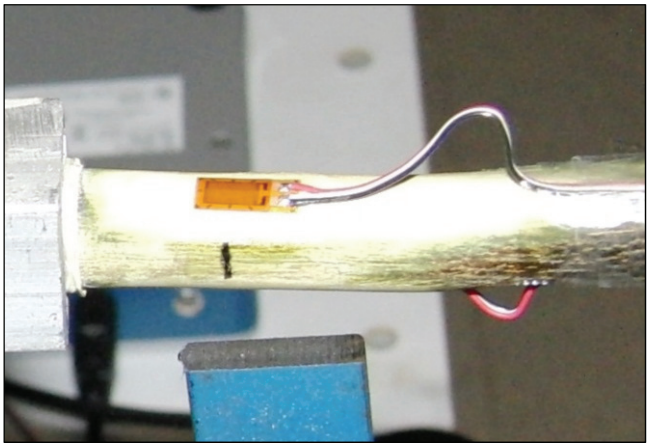

Figure 9. Close-up view of strain gauges installed on top and bottom surfaces of a branch specimen.

Mechanistic Models

The objective functions for the optimization of the shaker were formulated mathematically in terms of a mechanistic index. The mechanistic index is a function of one or more parameters of the objectives, which are structural response quantities that can be computed and correlated with the objectives. The indices are defined based on the demand versus the capacity of a system. The FEA outputs were used in the formulation of the mechanistic models.

Mechanistic Tree Damage Model

The goal of this study is to minimize the loss or injury of main tree limbs or scaffold branches having diameters larger than 6.35 cm (2.5 in.). For a citrus tree, damage to these tree limbs may result in the following:

- Damage can potentially reduce next year's fruit yield (Spann and Danyluk, 2010) because the maximum fruit bearing region of a citrus tree is largely supported by the main scaffold branches (Gupta et al., 2015); if

these branches break, they require significant time to grow back again.

- The tree injuries are potential sources of microbial and fungal infections that may infect whole tree.

During citrus harvesting with a canopy shaker, the primary limbs are subjected to cyclic bending loads every time the sinusoidally vibrating tines strike them. The repeated impacts cause cyclic bending stress in the limbs, but these stresses are not large enough to cause fatigue failure of the limbs. However, it was noted that the branches entangle between the tines and bend excessively as soon as the distance between them decreases because of the forward motion of the canopy shaker. The limbs first yield due to longitudinal bending stress, then buckle inward, and finally break by splitting along the transverse direction, as shown in figure 10. This failure scenario is simulated in the FEM by subjecting the branches to repeated impacts of tines that are simultaneously vibrating sinusoidally and moving forward linearly. The branches under stress are considered to be structurally damaged or to fail if the dynamic stresses and strains in the branches exceed the yield strength or modulus of rupture of the wood.

Consistent with the above failure mode, structural damage of a branch is estimated using a damage index in the numerical model. The damage index is expressed as the ratio of the maximum response of the limbs (δ_M) to the maximum allowable deformation or strength of the limbs (δ_U), as described in equation 3. Branches are said to fail when DI ≥ 1, whereas they are elastically deformed when DI < 1:

$$\mathrm{DI} = \frac{\delta_M}{\delta_U} \tag{3}$$

The structural damage response of each limb was expressed in terms of root mean square of the axial stress (S11). The stress (σ) is a vector of the maximum sectional axial stress (S11) computed at all the critical points in the damaged region for which $d \geq d_{critical}$, as given in equation 4, where i = 1, 2, 3, and 4, corresponding to the section points of the beam element. Figure 11 shows a branch limb with the critical region having a diameter of more than 6.35 cm (2.5 in.), as defined by a series of dots. The response of the

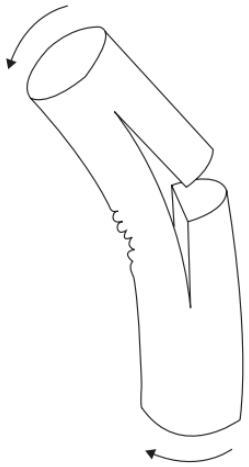

Figure 10. Failure mode of a branch under bending load.

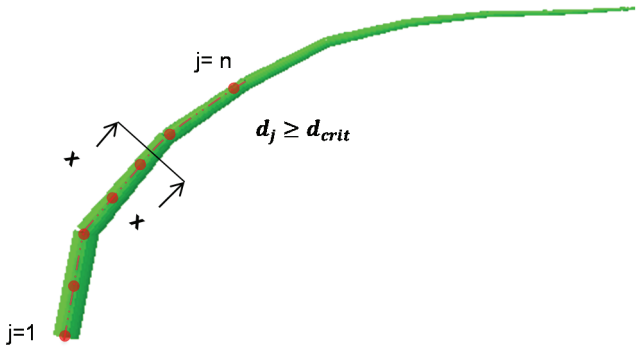

Figure 11. Finite element model of a tree limb in which red dots indicate critically damaged region.

individual limb prototypes (δ_m) is the maximum of a sectional stress (σ) for that limb, as given by equation 5. The damage index of individual limb prototypes is determined by normalizing the response of the limb by its capacity. The capacity is taken as the minimum of modulus of rupture (δ_U) of wood and maximum response of limb prototypes when analyzed with the current machine configuration (δ_S), as given in equation 6. The damage index of all limb prototypes in a tree zone was averaged to provide the damage index of that zone (DI), as given by equation 7, where k = 1, 2, 3,…, p (number of limb prototypes in a zone), and z = 1, 2, and 3, corresponding to the top, middle, and bottom zones, respectively:

$$\sigma = \max\left(\left\|\mathrm{Sl}\,1_i\right\|_2\right) \tag{4}$$

$$\delta_m = \max\left(\sigma_j\right) \tag{5}$$

$$D = \frac{\delta_m}{\min\left(\delta_S, \delta_U\right)} \tag{6}$$

$$\mathrm{DI}_z = \frac{1}{p}\sum_{k=1}^{p}\left|D_k\right| \tag{7}$$

Mechanistic Fruit Detachment Model

The canopy shaker is mainly used to mass harvest citrus crops for the processing industry, not the fresh market; therefore, no qualitative aspect of fruit harvesting is considered in the current study. The mechanism of fruit detachment has been investigated analytically and experimentally by Fridley and Adrian (1966), Wang and Shellenberger (1967), Cooke and Rand (1969), Diener et al. (1969), Liang et al. (1971), Parchomchuk and Cooke (1972), Miller and Morrow (1976), Berlage and Willmorth (1974), Savary (2009), and Savary et al. (2011). They found that the amount of fruit removed is highly correlated with acceleration of the fruits. The past studies have suggested that the ratio F/W (the tensile force required to detach the fruit divided by the fruit weight) is a good indicator of the amount of fruit detachment by shaking. The typical value of this ratio for fruits such as citrus and prunes varies from 1 to 50 depending on the fruit variety and size. Savary (2009) measured the force required to detach Hamlin and Valencia oranges. He concluded that an average static force of 96.1 N and an average shaking force of 17.1 N

are required to remove these fruit varieties. Therefore, a system that provides an acceleration of approximately 9 g would be more likely to detach citrus fruits based on the average weight of 0.186 kg. However, using this value to define the maximum capacity of the fruit detachment model would not be accurate owing to the high variability of fruit weight. Thus, the maximum possible amount of fruit removal (or capacity) is obtained by analyzing the acceleration of the fruit bearing region of the limb prototypes when simulated with the current configuration of the canopy shaker, which provides 96% to 99% in-field fruit detachment efficiency (Roka et al., 2008). The fruit bearing regions were defined, and the fruits were modeled as a lumped mass for each limb prototype in the FE analysis, as shown in figure 12.

The fruit detachment response (a^r) in the fruit bearing region of a limb prototype was computed as the root mean square of the resultant acceleration, as shown in equation 8. The fruit detachment response of an individual limb prototype (a_m), as shown in equation 9, was calculated as the mean of the responses in the fruit bearing region of the limb prototype. The fruit detachment index (FD) of a limb prototype was obtained by normalizing the fruit detachment response (a_m) by the response of the same limb prototype when simulated with the current tine configuration of a canopy shaker (a_s), as given in equation 10. The fruit detachment response of a zone (FDI) was obtained by taking the average of the fruit detachment indices of all the limb prototypes in a zone, as given by equation 11, where $k = 1, 2, 3, \ldots, p$ is the number of limb prototypes, and $z = 1, 2, 3$, corresponding to the top, middle, and bottom zones, respectively:

$$a^r = \left\| \left(\sqrt{a_x + a_y + a_z} \right) \right\|_2 \tag{8}$$

$$a_m = \frac{1}{n} \sum_{j=1}^{n} a^r \tag{9}$$

$$\mathrm{FD} = \frac{a_m}{a_S} \tag{10}$$

$$\mathrm{FDI}_z = \frac{1}{p} \sum_{k=1}^{p} \left| \mathrm{FD}_k \right| \tag{11}$$

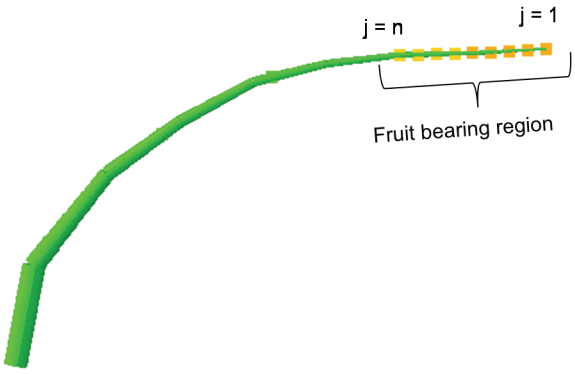

Figure 12. Finite element model of limb showing fruit bearing region.

Multi-Objective Optimization

Fruit detachment and tree damage depend on the amount of shaking energy transferred to the tree limbs by the harvester. The more energy transferred, the more fruits are removed; however, more energy may also result in more tree damage. Thus, an optimal machine parameter must be found to minimize the tree damage without compromising the fruit removal. Theoretically, the shaking energy associated with sinusoidal vibrating tines is given in equation 12:

$$E_s = \frac{1}{2} m \omega^2 A^2 \sin^2(\omega t - \varphi) \tag{12}$$

where m is mass, ω is angular frequency, A is amplitude, t is time, and φ is phase angle.

Instead of considering the shaking energy as a variable, its independent variables (i.e., frequency and amplitude) were chosen as design variables in the optimization because they can be independently controlled and physically altered to obtain the variable shaking energy.

In addition to the operating variables, the structural parameters of the tine (i.e., geometry and material), which determine how the tine interacts with branches and transmits the shaking energy from shaker to tree, are also considered as design variables in the optimization. A two-piece design of the experimental tine, as shown in figure 13, is proposed in this study. The design was chosen such that it would be inexpensive, could be tested using available laboratory equipment, and would be easy to adopt and implement in an existing harvester.

The proposed tine consists of the current design (i.e., a hollow steel pipe that forms the base and is attached to the hub of the canopy shaker) and an insert in the form of a solid rod or hollow tube. The stiffness (s), which is a function of the geometry and material of the insert, and the length of the insert in percentage (x) were defined as the design variables in the optimization of the shaker. The formulation for the optimization of the canopy shaker, developed in the following sections, is given in equation 13:

Find s, x, v, a:

$$\text{Minimize} \quad \mathrm{DI}(s,x,v,a) \tag{13a}$$

$$S \in \mathrm{R}^n(s),\ x \in \mathrm{R}^n(x),\ v \in \mathrm{R}^n(v),\ a \in \mathrm{R}^n(a)$$

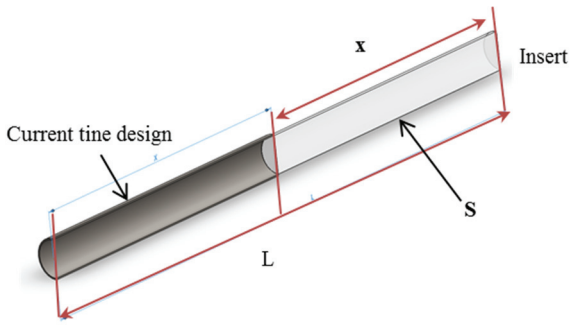

Figure 13. Proposed two-piece tine for adaptive shaking of canopy.

Table 1. Geometry and material configuration of various insert designs.

Geometry	Designation	Dimensions r_o (mm)	Dimensions t (mm)	Elastic Modulus, E (GPa)	Material Type
Solid rod	P1	18.98	0	3	Polyamide (PA), cast, molding and extrusion or 15% glass fiber reinforced
	P2	18.98	0	8	PA, 30% long glass fiber reinforced or 40% glass fiber and mineral fiber reinforced
	P3	18.98	0	14	PA, 50% long glass fiber reinforced
	P4	18.98	0	20	PA, 60% long glass fiber reinforced or 30% polyacrylonitrile (PAN) carbon fiber reinforced
	P5	18.98	0	28	PA, 50% PAN carbon reinforced
Hollow pipe	A6	20.64	1.5	80	Cast or wrought aluminum alloy
	A7	20.64	2.0	80	Cast or wrought aluminum alloy
	A8	20.64	2.5	80	Cast or wrought aluminum alloy
	A9	20.64	3.0	80	Cast or wrought aluminum alloy
Hollow pipe	D0 (current design)	20.64	1.65	210	Drawn over mandrel (DOM) 4130 steel

$$\text{Maximize} \quad S \in \mathrm{R}^n(s),\ x \in \mathrm{R}^n(x),\ v \in \mathrm{R}^n(v),\ a \in \mathrm{R}^n(a) \quad \text{FDI}(s,x,v,a) \tag{13b}$$

Subjected to:

Structural variables:

$$\underline{s} \le s_i \le \bar{s}, \forall i = 1,\ldots,n_s$$

$$\underline{x} \le x_j \le \bar{x}, \forall j = 1,\ldots,n_x$$

Operating variables:

$$\underline{v} \le v_k \le \bar{v}, \forall k = 1,\ldots,n_v$$

$$\underline{a} \le a_l \le \bar{a}, \forall l = 1,\ldots,n_a$$

Design of Experiments (or Design Domain)

The design of experiments (DOE) to predict optimal configurations of the machine was based on findings from past research and field experiments and included the following design variables:

Stiffness: The flexural stiffness of the insert (s) is a function of the geometry and material of the insert. The different designs of the insert were chosen based on market availability and the findings of the field tests performed by Oxbo International and Florida citrus growers. Different variants of polyamide (also called nylon) with the same cross-section (denoted P1 to P5) and different cross-sectional geometries of aluminum (denoted A6 to A9) were chosen for testing (table 1). The different variants of polyamide have different stiffness values based on their different fillers, such as carbon, silica, and minerals, and their percentage content in the polyamide. Figure 14 shows the variation of stiffness of the various designs of insert normalized to the stiffness of the current design.

Length of Insert: The length of an insert (x) is defined as the percentage length of the insert (P1 to P5 and A6 to A9) with respect to that of the current design (D0) in the proposed two-piece design, as shown in figure 13. Only twenty DOEs, as listed in table 2, were created for this design variable in order to appropriately balance the computational cost and degree of exploration in the design domain to find the optimal configuration. In table 2, the value of 0% for insert length means that the tine is the current design (hollow steel pipe), whereas the value of 100% means that the tine is completely composed of the new design (solid tube of PA or hollow tube of aluminum).

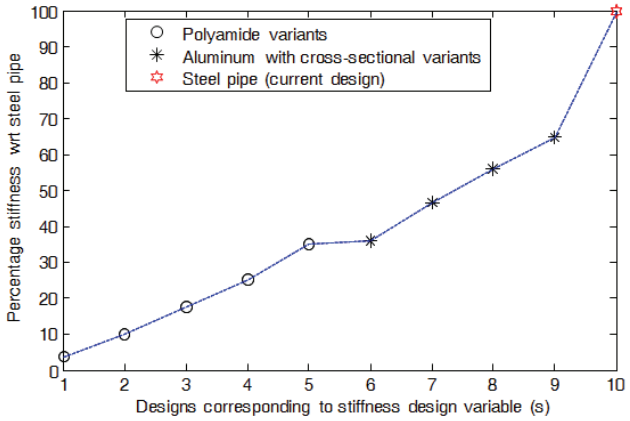

Figure 14. Variation of stiffness of multiple insert designs, normalized with respect to stiffness of the current tine design.

Table 2. Experiments for numerical analysis and optimization.

Design Variable	Lower Bound	Upper Bound	Design Values
Length of insert (x), %	0	100	0, 5, 100
Shaking frequency (v), Hz	2	8	2, 1, 8
Shaking amplitude (a), cm (in.)	2.54 (1)	15.24 (6)	2.5, 2.54, 15.24 (1, 1, 6)

Shaking Frequency and Shaking Amplitude: The shaking amplitude (a) determines the amount of flexural deformation that can be imparted to the tree limbs, and the shaking frequency (v) determines how many times and how soon the tine strikes the branches. Based on the experiments conducted on citrus crops using various mechanical harvesters, good harvesting results were achieved using a stroke of 10 to 12.5 cm (3.9 to 4.9 in.) at a frequency of 1.6 to 5.9 s^{-1} (O'Brien and Fridley, 1983). Thus, this range of frequency and amplitude was used to create the DOE listed in table 2.

Estimation of Analysis Time for Optimization

The total time for optimization is the FE analysis computation time multiplied by the number of iterations required in the optimization. The dynamic FE analysis of a tree limb prototype takes about 5 min. The total time required for the optimization of a single zone (i.e., the time required for FE simulations of all DOEs multiplied by the number of limb

prototypes) is approximately 138 days. This amount of computational time hardly justifies the practical value derived from such a long and tedious analysis. Additionally, the multidimensional optimization requires special techniques to find the optimal design, such as gradient-based optimization, genetic, and evolutionary algorithms. These techniques further require special programs as well as additional computational resources. Thus, a strategy was put forth to minimize the computational time by employing a classic graphical optimization technique instead of any special optimization algorithms. This strategy consists of solving the optimization problem in two phases: the first phase of optimization (phase I) involves only structural variables (s, x), while the second phase (phase II) uses the best designs of phase I to further improve the objective functions defined in terms of machine operating variables (v, a).

The proposed strategy has an additional advantage of being able to provide separate optimal designs based on changes in the structure of the machine and in the machine operating parameters. The structural parameters of a machine are easier to implement and test in the field as they only involve procurement of a new design of tines. However, machine operating parameters (i.e., a particular combination of frequency and amplitude) require changes to the vibratory mechanism. In the case of a citrus canopy harvester, the frequency can be adjusted easily, but amplitude adjustments require changing the slider crank mechanism. In addition, to accomplish variable shaking of the tree canopy, the three different shaking parameters of the tine require three different vibratory mechanisms to be built into the machine. Therefore, modifying the design based on the operating parameters would be significantly costlier and more difficult to implement in an existing machine. However, they result in significant improvement in the performance of the canopy shaker.

SHAKER OPTIMIZATION: PHASE I

Phase I involves the optimization of the shaker based only on structural variables: stiffness (s) and percentage length of the insert (x). The operating variables were fixed to the current machine setting with a frequency (v^0) and amplitude (a^0) of 4 Hz and 10.16 cm (4 in.), respectively. The following procedure was adopted to find the optimal tine configuration for each zone:

- The dynamic response of the limb prototypes for each zone was computed using FE analysis.
- The fruit detachment index and damage index were calculated for each zone using mechanistic models.
- Pareto frontiers were constructed for each zone to determine the optimal design. The Pareto frontiers were constructed based on the dominance principle in which a set of non-dominated design points are chosen such that no objectives can be further improved without impairing the other. The Matlab program designed by Freitas (2012) was used to create the Pareto frontiers.
- To minimize the computational cost, the bi-objective formulation was converted into the mono-objective by converting the fruit detachment index into the constraint, as shown in equation 14. The Pareto-optimal design was selected to obtain at least a 15% reduction in tree damage:

$$\begin{aligned} &\text{Minimum}\left(\text{DI}-0.85\right) \\ &\text{FDI}-\text{FDI}_{Allowable}\geq 0 \end{aligned} \tag{14}$$

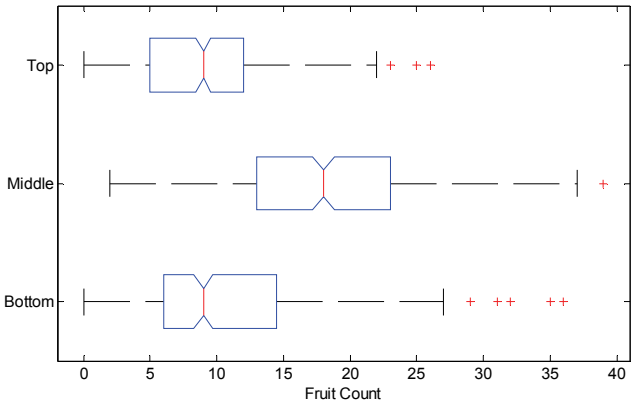

Figure 15. Distribution of citrus fruits in three zones of canopy.

Table 3. Allowable fruit detachment index.

Top zone	0.8
Middle zone	0.9
Bottom zone	0.8

The value of $\text{FDI}_{Allowable}$ was chosen based on the fruit distribution in a citrus tree. The fruit harvesting efficiency can be increased by providing a large shaking force to the parts of canopy that have comparatively large numbers of fruits. In the current study, the fruit harvesting efficiency is achieved by setting a high value of $\text{FDI}_{Allowable}$ to the fruiting zones. Whitney and Wheaton (1984) studied the fruit distribution pattern of citrus trees and concluded that most of the fruiting occurs in the middle and outer parts of the canopy. To corroborate their findings for medium-size citrus trees, an experiment was planned, and fruit distribution was analyzed for 361 trees. Figure 15 shows the distribution of fruits in the three zones of a tree canopy. It was found that the average fruit density in the middle zone of a tree canopy is twice that in the top and bottom zones. Thus, the overall harvesting efficiency can be improved by setting a higher value of $\text{FDI}_{Allowable}$ for the middle zone than for the bottom and top zones. The values of $\text{FDI}_{Allowable}$ selected for phase I of the optimization for each zone of a tree canopy are listed in table 3.

SHAKER OPTIMIZATION: PHASE II

In phase II, the shaker was further improved by setting the optimal combination of operating parameters: frequency (v) and amplitude (a). The best designs of phase I were used to find the optimal operating parameters. The following procedure was adopted in this phase of optimization:

- Dynamic analysis was performed for the DOEs to construct the response surface for the objective functions.
- Radial basis neural network (RBNN; Park and Sandberg, 1991) was used to construct the analytical response surface of the fruit detachment index and the damage index as a function of two design variables:

shaking frequency and amplitude. The Matlab program designed by Viana (2010) was used to construct the RBNN response surface. The parameters of the RBNN were chosen based on the minimum $PRESS_{RMS}$.

- The FDI and DI were computed for each combination of frequency and amplitude as defined in the DOE setup.
- The Pareto frontiers for the best designs of each zone were constructed from the FDI and DI response surfaces.
- The best operating combination of frequency and amplitude was determined using equation 15:

$$\begin{aligned} &\text{Minimum DI} \\ &\text{FDI} - \text{FDI}_{Allowable} \geq 0 \end{aligned} \tag{15}$$

Results and Discussion

The validated FEA model was used to find the dynamic response of the tree limb prototypes. The dynamic responses of the tree limbs were used to formulate mechanistic models, which were then used in a two-stage optimization to minimize tree damage and maximize fruit detachment.

Finite Element Model Verification

The objective functions, defined in terms of accelerations and strains, were computed and compared with experiments to validate the FE model. Figures 16 and 17 show comparisons of the strain and acceleration computed from the FE model with the experimental results. The regression line of the root mean square (RMS) of the longitudinal strains along the branch has a slope of 0.7394, an intercept of 0.0002, and an R^2 of 0.93. The regression line for the RMS of acceleration has a slope of 0.9392, an intercept of 5.1932 m s^{-2}, and an R^2 of 0.85. The results show that the longitudinal strains and accelerations computed from the FE model and from the experiments are highly correlated, having respective Pearson coefficients of 0.97 and 0.92. Thus, the FE model was able to predict the mechanical behavior of the branch with acceptable accuracy under the dynamic impact loading conditions; therefore, similar FE parameters were used to analyze the tree limb prototypes for optimization of the canopy shaker. Since RMS values of acceleration and strain were used to validate the FEA model, the same measures were used in defining the canopy shaker objective functions over a period of cyclic loading.

Phase I Optimization

This section presents the results obtained in phase I of the optimization. Three different optimal configurations of tines are proposed, corresponding to three zones of the citrus canopy. Any tine design can be selected from the proposed optimum designs and incorporated into the canopy shaker based on the amount of improvement needed and the amount of expenditures one is willing to invest.

Tine Set II for Middle Zone of Canopy

Figure 18 shows the Pareto front between the two objective functions, i.e., damage index (DI) and fruit detachment index (FDI), for the middle zone of the citrus canopy. For

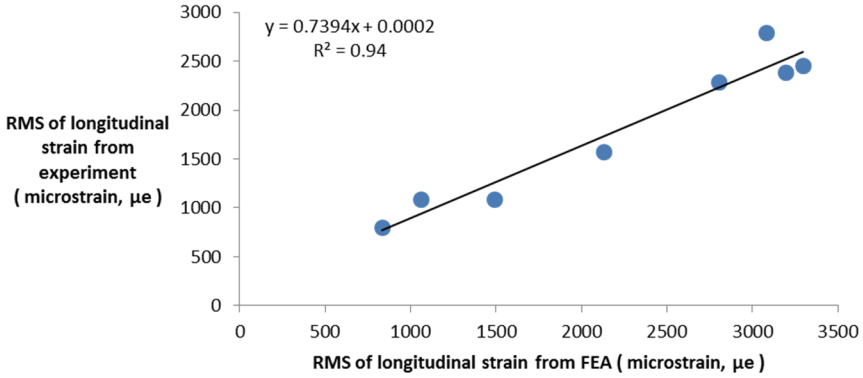

Figure 16. Comparison of RMS of maximum strain of the branch specimen obtained from FE analysis and from experiments.

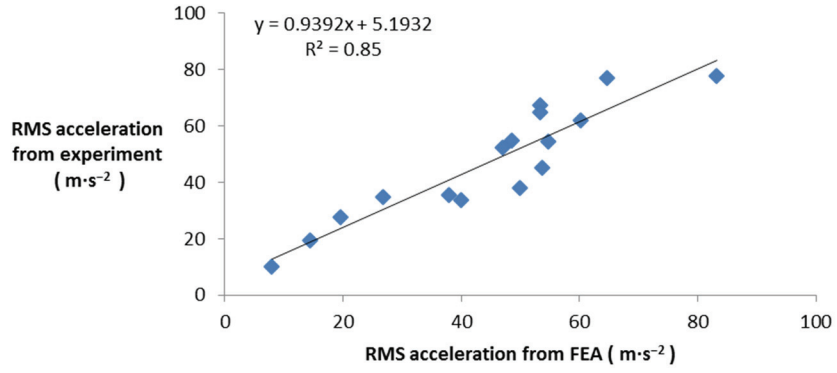

Figure 17. Comparison of RMS of acceleration of the branch specimen obtained from FE analysis and from experiments.

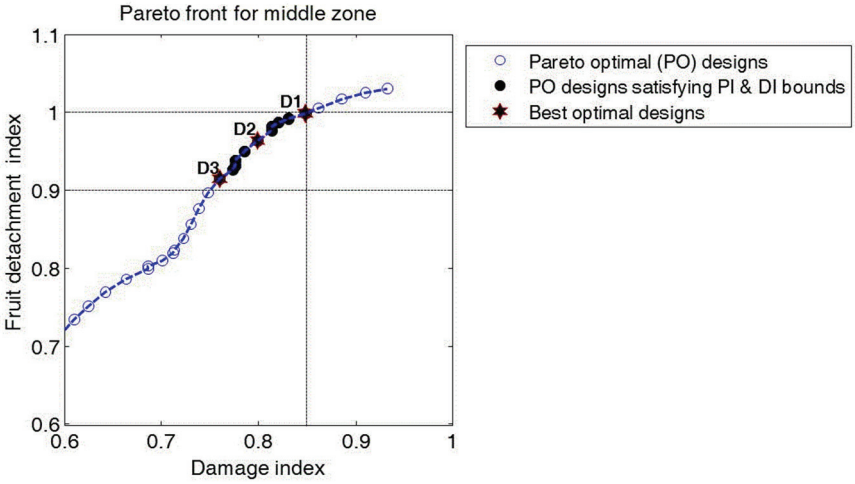

Figure 18. Pareto front to predict the optimum designs for tine set II of the middle zone of the citrus canopy.

Table 4. Selected optimal configurations for tine set II of the canopy shaker.

Tine Set	Zone	Best Designs	Tine Configuration	Reduction in Damage (%)	Fruit Detachment (%)
II	Middle	D1: Configuration P5	70% 28 GPa PA	15.2	100.0
		D2: Configuration P4	70% 20 GPa PA	20.1	96.4
		D3: Configuration P3	65% 14 GPa PA	24.0	91.5

the middle zone, the upper bound on DI and the lower bound on FDI were set to select only those designs that resulted in at least a 15% reduction in tree damage and a minimum fruit detachment index of 90%. Three optimal tine designs were selected as the best candidates over all the criteria-satisfying designs for tine set II (defined in fig. 2) of the canopy shaker. These designs, listed in table 4, are design D1 with the highest FDI, design D3 with highest reduction in tree damage, and design D2 having a fruit detachment index and reduction in tree damage between those of D1 and D3. This study proposes only three tine designs for the middle section of the canopy shaker based on the trade-off between cost and the amount of improvement needed because the cost of the stiffer polyamide P5 (E - 28 GPa as shown in table 1) is approximately eight times that of P3 (E - 14 GPa) polyamide (Gupta, 2013).

In design D1, the tine configuration of 70% for design P5 (28 GPa nylon) means that the tine was composed of 70% length of the new insert (P5) and 30% length of the current design (D0). This design is proposed to result in a 15.2% reduction in tree damage and approximately 100% fruit removal. This means that a canopy shaker with this tine design will induce 15% less stress on the primary limbs, and thus less damage. In addition, this design is estimated to provide the same amount of fruit removal as the current tine design. In the field, the current configuration of tines has resulted in fruit harvesting efficiencies of 94% to 96% (Roka et al., 2008). A significant amount of reduction in tree damage can also be accomplished by using designs D2 and D3; however with comparatively lower fruit removal.

Tine Sets I and III for Top and Bottom Zones of Canopy

Figure 19 shows the Pareto fronts for the top and bottom zones of the citrus tree canopy. The top and bottom zones of the canopy have a high density of scaffold branches, and damage to them adversely affect the next year's fruit yield. Therefore, the optimal tine designs were selected to accomplish a greater reduction in tree damage (more than 20%, as defined in eq. 15) compared to the middle zone. Two optimal designs (D1 and D2) and three optimal designs (D1, D2, and D3), as listed in table 5, were selected as the best optimum candidates for tine set I and tine set III of the canopy shaker, respectively. Design D1 of tine set I resulted in 102% fruit detachment in the top zone; this simply means that the average acceleration of the fruit bearing region of the limbs in the top zone is 2% more than could be obtained with the current design, D0. Physically, a fruit detachment index of >100% means that there is a higher probability of achieving a harvesting efficiency of 100% during citrus harvesting. A substantial reduction in tree damage of approximately 30% to 35% for the top and bottom zones of the canopy shaker can also be achieved by using D2 for tine set I and D3 for tine set III. However, it may result in 15% to 20% reduction in fruit removal. This reduction in fruit removal can be accepted because of the significantly fewer fruits in the top and bottom zones as compared to the middle zone of the tree canopy.

PHASE II OPTIMIZATION

Phase II of the optimization resulted in different combinations of frequency and amplitude to further minimize tree damage and maximize fruit removal. From a manufacturing point of view, these combinations of frequency and amplitude are obtained by employing three different vibratory mechanisms in the harvesting system, corresponding to the three zones of the tree canopy. The cost of installing these modifications could be high but should be considered owing to the improvement achieved. The optimal operating parameters of a canopy shaker for each tine set corresponding to its zone are presented in the following sections.

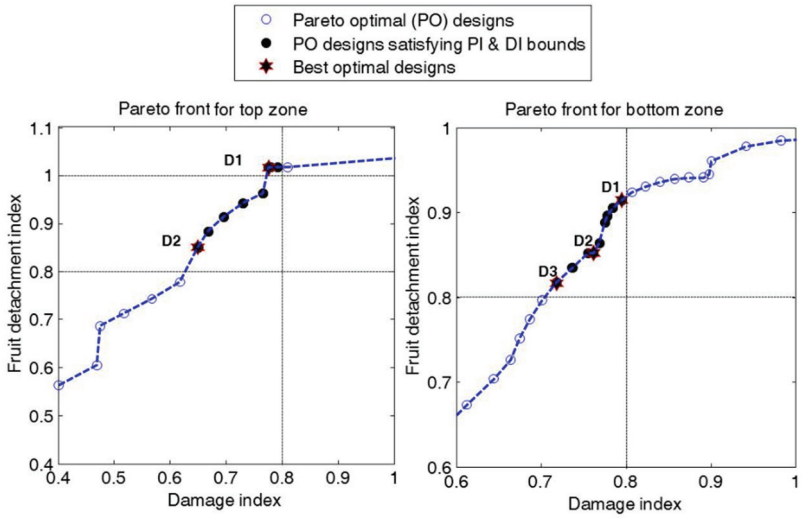

Figure 19. Pareto fronts to predict the optimum designs of tine set I for top zone (left) and tine set III bottom zone (right) of the citrus canopy.

Table 5. Selected optimal configurations for tine set I and III of the canopy shaker.

Tine Set	Tree Zone	Best Designs	Tine Configuration	Reduction in Damage (%)	Fruit Detachment (%)
I	Top	D1: Configuration P5	100% 28 GPa PA	22.5	102.0
		D2: Configuration P4	100% 20 GPa PA	35.0	85.0
III	Bottom	D1: Configuration P5	80% 28 GPa PA	20.6	91.5
		D2: Configuration P4	80% 20 GPa PA	23.8	85.2
		D3: Configuration P3	70% 14 GPa PA	28.2	81.7

Table 6. Optimal operating parameters for the selected designs for tine set II of the canopy shaker.

Best Designs (Phase I)	Frequency (Hz)	Amplitude, cm (in)	Reduction in Damage (%)	Fruit Detachment (%)
D1 and D3	7.8	3.81 to 5.08 (1.5 to 2)	30 to 20	90 to 100
D2	3.6	11.68 (4.6)	20	102
	6.4	5.08 (2)	26	91

Tine Set II for Middle Zone of Canopy

The optimal operating parameters for the best designs (D1, D2, and D3) for tine set II, as listed in table 6, were selected to obtain a minimum fruit removal of 90%. It is evident from table 6 that designs D1 and D3, when operated at a high frequency of approximately 7.8 s^{-1} and low amplitude of 3.81 to 5.08 cm (1.5 to 2 in.), resulted in a 20% to 30% reduction in tree damage and 90% to 100% fruit removal. For D2, two different optimal combinations of frequency and amplitude were found. At a high frequency of around 6.5 s^{-1} and a low amplitude of 5.08 cm (2 in.), a 26% reduction in tree damage with approximately 91% fruit removal was computed; however, decreasing the frequency to 3.6 s^{-1} and increasing the amplitude to 11.68 cm (4.6 in.) resulted in a 20% reduction in tree damage with more than 100% fruit removal.

Tine Set I for Top Zone of Canopy

The optimal operating parameters for the best designs for tine set I of the canopy shaker are listed in table 7. A high frequency in the range of 6.5 to 7.5 s^{-1} and a mid-range amplitude of 7.62 to 8.89 cm (3 to 3.5 in.) for both the optimal designs (D1 and D2) for tine set I was estimated to provide 40% to 55% reduction in tree damage and more than 100% fruit removal.

Table 7. Optimal operating parameters for the selected designs for tine set I of the canopy shaker.

Best Designs (Phase I)	Frequency (Hz)	Amplitude, cm (in.)	Reduction in Damage (%)	Fruit Detachment (%)
D1 and D2	6.5 to 7.5	7.62 to 8.89 (3 to 3.5)	40 to 55	>100

Tine Set III for Bottom Zone of Canopy

The optimal operating parameters and improvement in the objective functions for the best designs for tine set III, which mainly interacts with the bottom section of the tree canopy, are listed in table 8. Two optimal combinations of frequency and amplitude were observed for designs D2 and D3. These tine configurations, when operated at the mid-range frequency of 3 to 3.5 s^{-1} and high amplitude of 13.97 to 15.24 cm (5.5 to 6 in.), were estimated to provide 35% to 40% reduction in tree damage and 80% fruit detachment from the bottom section of the tree canopy. However, approximately 100% fruit detachment was estimated at the high frequency of 7.5 s^{-1} and low amplitude of approximately 6.35 cm (2.5 in.) with a 20% to 25% reduction in tree damage. Design D1, at an optimal frequency of 3 to 3.5 s^{-1} and amplitude of 13.97 to 15.24 cm (5.5 to 6 in.), was computed to provide an approximately 35% reduction in tree damage and only 80% fruit removal.

Table 8. Optimal operating parameters for the selected designs for tine set III of the canopy shaker.

Best Designs (Phase I)	Frequency (Hz)	Amplitude, cm (in.)	Reduction in Damage (%)	Fruit Detachment (%)
D1, D2, and D3	3 to 3.5	13.97 to 15.24 (5.5 to 6)	35 to 40	~80
D2 and D3	7.5	6.35 (2.5)	20 to 25	~100

Summary of Results

The goal of this research was to find the optimal machine parameters that can provide variable shaking energy to the different sections of the tree canopy to maximize fruit removal and minimize tree damage. The shaking energy associated with the tine, which is a function of the tine mass, frequency, and amplitude of vibration, was calculated using equation 12 and plotted against the damage index for all the optimal designs, as shown in figure 20. The shaking energy was normalized with the current design of the canopy shaker (D0) to compare the proposed designs. As highlighted earlier, most of the fruiting occurs in the middle section of the tree, and most of the scaffold branches are in the bottom section; therefore, the damage index values are plotted to obtain a minimum of 100% FDI for the middle and top sections and 80% for the bottom section. The current design (D0) shakes the limbs with a higher shaking energy to obtain fruit removal of 95% to 99% in the field. This in turn results into higher stresses on the branches, and thus more damage to the tree. As shown in figure 20, the optimized designs, which are comparatively 50% to 70% less stiff (fig. 14) than the current design, were able to achieve the same amount of fruit removal by applying less shaking energy to the tree limbs, and thereby less damage to the tree. In addition, the optimized designs are variants of polyamide, which is softer, with a hardness of D80 (on the Durometer scale), than the current tine design, which is made of DOM 4130 steel and has a hardness of C-13 on the Rockwell scale (source: Oxbo International, Shipshewana, Ind.). The optimized designs provide relatively soft and cushioned impacts on the tree limbs during shaking and thus produce less abrasion or injury to the limbs. This was also confirmed during the on-site trials by replacing the steel tines of the canopy shaker with polyamide rods and visually inspecting the abrasion on the trees.

Limbs that are long, thick, and curved toward the ground due to the weight of fruits are typically observed in the middle section of the tree canopy. These limbs are the maximum fruit bearing branches, and an optimal design should reduce the stresses on them in order to have higher fruit yield. It was found that changing the tines in tine set II to a moderately stiffer material (D1 and D3 in table 4) and configuring them to vibrate at a high frequency of 7.8 s^{-1} and amplitude of 3.81 to 5.08 cm (1.5 to 2 in.) provided a shaking energy that was 55% to 80% less than that of the current design. This is estimated to result a reduction of the stress on the limbs in the middle section of the canopy of approximately 20% to 25% without reducing fruit removal efficiency.

However, the limbs in the bottom section of the canopy are more rigid and vibrate less than those in the middle section; therefore, they require more shaking energy to achieve the same fruit removal as compared to the middle section. Since the bottom section has fewer fruits and the thickest branches support and nurture the whole tree, the optimal designs are proposed to target only 80% fruit removal and minimize the tree damage as much as possible. Thus, the optimal designs (D1, D2, and D3 in table 5) for tine set III when vibrated at the optimal frequency of 3 to 3.5 Hz and amplitude of 13.97 to 15.24 cm (5.5 to 6 in.) provided 35% to 60% less energy to the tree as compared to the current design. This resulted in a 30% to 50% reduction in the stress on the tree limbs and approximately 80% fruit removal.

Tine set I of the canopy shaker interacts with the top section of the citrus canopy, which has limbs that are long and thin, grow straight up to a height of 2.54 to 3.3 cm (100 to 130 in.), and then curve downward slightly. These limbs are flexible and behave like long thin cantilever beams, but they can break under a sudden impact from the tine due to high localized stresses. Thus, changing the current design to one that has low stiffness, such as a solid rod of polyamide reinforced with 60% long glass fiber or 30% PAN carbon, and that vibrates at a frequency of 6.5 to 7.5 s^{-1} and amplitude of 7.62 to 8.89 cm (3 to 3.5 in.) would provide 50% to 70% less shaking energy as compared to the current design and therefore result in a 40% to 55% reduction in tree damage. However, at these operating conditions, the optimal tine design provides sufficient energy to obtain approximately 100% fruit removal from the top section of the citrus canopy.

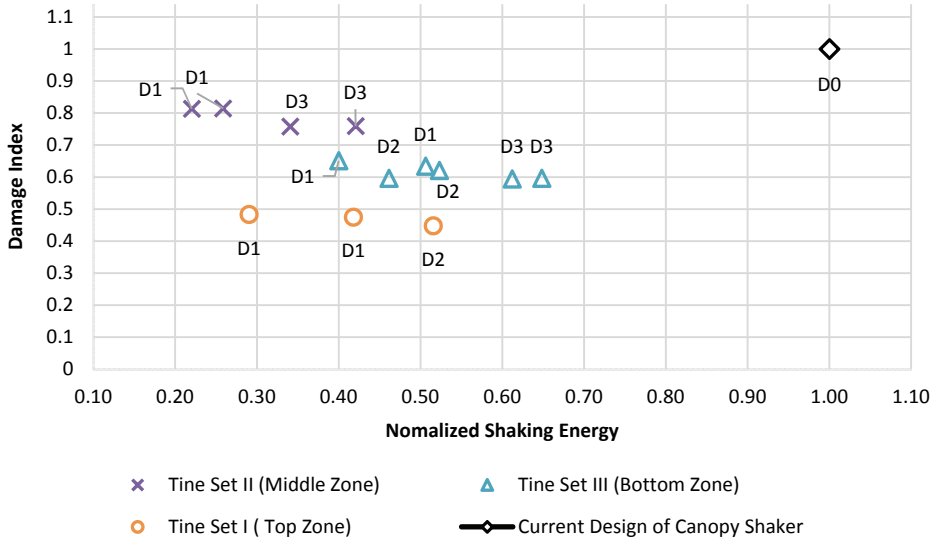

Figure 20. Comparison of damage index values of the optimal designs for three zones with shaking energy normalized to the current design.

Conclusions and Future Work

The main goal of this study was to provide an overview of the analytical possibilities available to improve the performance of vibratory citrus harvesters. The goal was pursued by employing numerical-based design optimization of a shaker system. Statistical modeling, objective function quantification using mechanistic modeling, response surface methods, and Pareto-optimal solution search techniques were applied to obtain optimal design solutions. The proposed design methodology represents an alternative to improve continuous canopy shakers based on variable shaking of the tree canopy. Although the proposed framework was devised for the optimization of citrus canopy shakers, it can be easily and effectively applied to the design and optimization of other fruit crops and harvesters.

In future work, the proposed designs will be evaluated in field trials to determine their efficacy. After evaluation, judgment will be made to determine which optimal machine configurations should be chosen for commercial harvesting of citrus. The possibility of redesigning a harvester may be explored further based on the experimental results and the theoretical model. The theoretical model, verified in the controlled environment of laboratory experiments, may be refined further depending on its correlation with the field trials. The following recommendations are suggested to further improve the canopy shaker and validate and refine the proposed analytical model to optimize other similar harvesters:

- A small-scale fruit removal system that works on principles similar to a continuous citrus canopy harvester should be built to validate the outcomes of current simulations.
- Field experiments should be planned to evaluate the proposed design modifications and refine the proposed analytical model.
- The effects of vertical shaking of a tree canopy can also be explored using numerical simulation.

Acknowledgements

The authors greatly acknowledge the Citrus Initiatives of Florida for providing research funding. We are also grateful to Dr. Peter Ifju, Dr. Arthur Teixeira, Sherrie Buchanon, Ali Mirzakhani, and Roy Sweeb for providing guidance related to material testing and data collection.

References

Arora, J. S., Elwakeil, O. A., Chahande, A. I., & Hsieh, C. C. (1995). Global optimization methods for engineering applications: A review. *Struct. Optimization, 9*(3), 137-159. http://dx.doi.org/10.1007/bf01743964

ASTM. (2014). E1237-93: Standard guide for installing bonded resistance strain gages. West Conshohocken, Pa.: ASTM.

Baier, H. (1977). Über algorithmen zur ermittlung und charakterisierung Pareto-optimaler lösungen bei entwurfsaufgaben elastischer tragwerke. *Z. Angew. Math. Mech., 57*(22), 318-320.

Bathe, K. J. (1996). *Finite element procedures in engineering analysis.* Englewood Cliffs, N.J.: Prentice-Hall.

Berlage, A. G., & Willmorth, F. M. (1974). Fruit removal potential of high-frequency vibrations. *Trans. ASAE, 17*(2), 233-234. http://dx.doi.org/10.13031/2013.36830

Carmichael, D. G. (1980). Computation of Pareto optima in structural design. *Intl. J. Numer. Methods Eng., 15*(6), 925-929. http://dx.doi.org/10.1002/nme.1620150610

Cheng, F. Y., & Li, D. (1998). Genetic algorithm development for multiobjective optimization of structures. *AIAA J., 36*(6), 1105-1112. http://dx.doi.org/10.2514/2.488

Choi, K. K., & Kim, N. H. (2005a). *Structural sensitivity analysis and optimization I: Linear systems.* New York, N.Y.: Springer.

Choi, K. K., & Kim, N. H. (2005b). *Structural sensitivity analysis and optimization II: Nonlinear systems and applications.* New York, NY: Springer.

Cooke, J. R., & Rand, R. H. (1969). Vibratory fruit harvesting: A linear theory of fruit stem dynamics. *J. Agric Eng. Res., 14*(3), 195-209.

Das, I., & Dennis, J. E. (1997). A closer look at drawbacks of minimizing weighted sums of objectives for Pareto set generation in multicriteria optimization problems. *Struct. Optimization, 14*(1), 63-69. http://dx.doi.org/10.1007/bf01197559

Das, I., & Dennis, J. E. (1998). Normal-boundary intersection: A new method for generating the Pareto surface in nonlinear multicriteria optimization problems. *SIAM J. Optim., 8*(3), 631-657. http://dx.doi.org/10.1137/S1052623496307510

Deb, K. (2001). *Multiobjective optimization using evolutionary algorithms.* New York, N.Y.: Wiley.

Diener, R. G., Levin, J. H., & Whittenberger, R. T. (1969). Relation of frequency and length of shaker stroke to the mechanical harvesting of apples. ARS 42-148. Washington, D.C.: USDA.

FASS. (2013). Florida citrus statistics 2011-2012. Tallahassee. Fla.: Florida Agricultural Statistics Service. Retrieved from https://www.nass.usda.gov/Statistics_by_State/Florida/Publications/Citrus/cit/2011-12/cit1011.pdf

Freescale. (2008). ±1.5 g - 6 g three-axis low-g micromachined accelerometer. Document No. MMA7260QT. Austin, Tex.: Freescale Semiconductor. Retrieved from www.freescale.com/files/sensors/doc/data_sheet/MMA7260QT.pdf

Freitas, A. D. (2012). Pareto fronts according to dominance relation. Natick, Mass.: MathWorks. Retrieved from www.mathworks.com/matlabcentral/fileexchange/37080-pareto-fronts-according-to-dominance-relation

Fridley, R. B., & Adrian, P. A. (1966). Mechanical harvesting equipment for deciduous tree fruits. Bulletin 825. Berkeley, Cal.: California Agricultural Experiment Station.

Fridley, R. B., & Yung, C. (1975). Computer analysis of fruit detachment during tree shaking. *Trans. ASAE, 18*(3), 409-415. http://dx.doi.org/10.13031/2013.36599

Gupta, S. K. (2013). Optimization of citrus harvesting system based on mechanistic tree damage and fruit detachment model. MS thesis. Gainesville, Fla.: University of Florida, Department of Mechanical and Aerospace Engineering.

Gupta, S. K., Ehsani, R., & Kim, N. H. (2015). Optimization of a citrus canopy shaker harvesting system: Properties and modeling of tree limbs. *Trans. ASABE, 58*(4), 971-985. http://dx.doi.org/10.13031/trans.58.10818

Hilber, H. M., Hughes, T. J. R., & Taylor, R. L. (1977). Improved numerical dissipation for time integration algorithms in structural dynamics. *Earthquake Eng. Struct. Dynamics, 5*(3), 283-292. http://dx.doi.org/10.1002/eqe.4290050306

Hughes, T. J. R. (1987). *Finite element method: Linear static and dynamic finite element analysis.* Englewood Cliffs, N.J.: Prentice-Hall.

Kim, N. H., & Shankar, B. V. (2009). *Introduction to finite element analysis and design.* New York, N.Y.: Wiley.

Koski, J. (1979). Truss optimization with vector criterion. Report

No. 6. Tampere, Finland: Tampere University of Technology.
Koski, J. (1980). Truss optimization with vector criterion, examples. Report No 7. Tampere, Finland: Tampere University of Technology.
Kristensen, E. S., & Madsen, N. F. (1976). On the optimum shape of fillets in plates subjected to multiple in-plane loading cases. *Intl. J. Numer. Methods Eng., 10*(5), 1007-1019. http://dx.doi.org/10.1002/nme.1620100504
Leitmann, G. (1977). Some problems of scalar and vector-valued optimization in linear viscoelasticity. *J. Optimization Theory Appl., 23*(1), 93-99. http://dx.doi.org/10.1007/bf00932299
Liang, T., Lewis, D. K., Wang, J. K., & Monroe, G. E. (1971). Random function modeling of macadamia nut removal by multiple frequency vibration. *Trans. ASAE, 14*(6), 1175-1179.
Lybas, J., & Sozen, M. A. (1977). Effect of beam strength ratio on dynamic behavior of reinforced concrete coupled walls. Report SRS No. 444. Urbana, Ill.: University of Illinois.
Marler, R. T., & Arora, J. S. (2004). Survey of multi-objective optimization methods for engineering. *Struct. Multidiscip. Optim., 26*(6), 369-395. http://dx.doi.org/10.1007/s00158-003-0368-6
Mayer, H. (1987). Wind-induced tree sways. *Trees, 1*(4), 195-206. http://dx.doi.org/10.1007/bf01816816
Messac, A., Ismail-Yahaya, A., & Mattson, C. A. (2003). The normalized normal constraint method for generating the Pareto frontier. *Struct. Multidiscip. Optim., 25*(2), 86-98. http://dx.doi.org/10.1007/s00158-002-0276-1
Miller, W. M., & Morrow, C. T. (1976). Vibrational characterization of the apple-stem system with respect to stem separation. *Trans. ASAE, 19*(3), 409-411. http://dx.doi.org/10.13031/2013.36039
Moore, J. R. (2002). Mechanical behavior of coniferous trees subjected to wind loading. PhD diss. Corvallis, Ore.: Oregon State University.
Myers, R. H., & Montgomery, D. C. (2002). *Response surface methodology: Process and product optimization using designed experiments* (2nd ed.). New York, N.Y.: Wiley.
O'Brien, M., & Fridley, R. B. (1983). *Principles and practices for harvesting and handling fruits and nuts.* Westport, Conn.: AVI.
Parchomchuk, P., & Cooke, J. R. (1972). Vibratory harvesting: An experimental analysis of fruit-stem dynamics. *Trans. ASAE, 15*(4), 598-603. http://dx.doi.org/10.13031/2013.37964
Pareto, V. (1906). Manuale di economica politica. Milan, Italy: Societa Editrice libraria. Translated into English by A.S. Schwier as Manual of political economy (A. S. Schwier and A. N. Page, Eds). 1971. New York, N.Y.: A. M. Kelley.
Park, J., & Sandberg, I. W. (1991). Universal approximation using radial-basis-function networks. *Neural Computation, 3*(2), 246-257. http://dx.doi.org/10.1162/neco.1991.3.2.246
Park, Y. J., & Ang, A. H. (1985). Mechanistic seismic damage model for reinforced concrete. *J. Struct. Eng., 111*(4), 722-739. http://dx.doi.org/10.1061/(ASCE)0733-9445(1985)111:4(722)
Pedersen, P., & Laursen, C. L. (1983). Design for minimum stress concentration by finite elements and linear programming. *J. Struct. Mech., 10*(4), 376-391.
Phillips, A. L., Hutchinson, J. R., & Fridley, R. B. (1970). Formulation of forced vibrations of tree limbs with secondary branches. *Trans. ASAE, 13*(1), 138-142. http://dx.doi.org/10.13031/2013.38553
Powell, G. H., & Allahabadi, R. (1988). Seismic damage prediction by deterministic methods: Concepts and procedures. *Earthquake Eng. Struct. Dynamics, 16*(5), 719-734. http://dx.doi.org/10.1002/eqe.4290160507
Roka, F., Burns, J., Syvertsen, J., & Ebel, R. (2008). Benefits of an abscission agent in mechanical harvesting of citrus. Document No. FE752. Gainesville, Fla.: University of Florida IFAS.
Roufaiel, M. S. L., & Meyer, C. (1987). Analytical modeling of hysteretic behavior of R/C frames. *J. Struct. Eng., 113*(3), 429-444. http://dx.doi.org/10.1061/(ASCE)0733-9445(1987)113:3(429)
Santos, J. L. T., & Choi, K. K. (1989). Integrated computational considerations for large-scale structural design sensitivity analysis and optimization. In H. A. Eschenauer, & G. Thierauf (Eds.), *Discretization methods and structural optimization: Procedures and applications* (pp. 299-307). Berlin, Germany: Springer. http://dx.doi.org/10.1007/978-3-642-83707-4_38
Savary, S. K. J. U. (2009). Study of the force distribution in the citrus canopy during harvest using continuous canopy shaker. MS thesis. Gainesville, Fla.: University of Florida, Department of Agricultural and Biological Engineering.
Savary, S. K. J. U., Ehsani, R., Salyani, M., Hebel, M. A., & Bora, G. C. (2011). Study of force distribution in the citrus tree canopy during harvest using a continuous canopy shaker. *Comput. Electron. Agric., 76*(1), 51-58. http://dx.doi.org/10.1016/j.compag.2011.01.005
Savary, S. K. J. U., Ehsani, R., Schueller, J. K., & Rajaraman, B. P. (2010). Simulation study of citrus tree canopy motion during harvesting using a canopy shaker. *Trans. ASABE, 53*(5), 1373-1381. http://dx.doi.org/10.13031/2013.34892
Spann, T. M., & Danyluk, M. D. (2010). Mechanical harvesting increases leaf and stem debris in loads of mechanically harvested citrus fruit. *HortSci., 45*(8), 1297-1300
Stadler, W. (1988). Fundamentals of multicriteria optimization. In W. Stadler (Ed.), *Multicriteria optimization in engineering and in the sciences* (pp. 1-25). Boston, Mass.: Springer. http://dx.doi.org/10.1007/978-1-4899-3734-6_1
Veletsos, A. S., & Newmark, N. M. (1960). Effect of inelastic behavior on the response of simple systems to earthquake motions. In *Proc. 2nd World Conf. Earthquake Eng., Vol. 2* (pp. 895-912). Tokyo, Japan: Science Council of Japan.
Viana, F. A. C. (2010). SURROGATES Toolbox User's Guide. Retrieved from https://sites.google.com/site/srgtstoolbox/
Wang, J. K., & Shellenberger, F. A. (1967). Effects of cumulative damage due to stress cycles on selective harvesting of coffee. *Trans. ASAE, 10*(2), 252-255.
Whitney, J. D., & Wheaton, T. A. (1984). Tree spacing affects citrus fruit distribution and yield. *Proc. Florida State Hort. Soc., 97*, 44-47.